EasyChair Preprint

№ 9566

Robotic Control for Vibration Reduction of Swinging Products

Robbert van der Kruk, Arend Jan van Noorden, Tom Oomen, Rene van de Molengraft and Herman Bruyninckx

January 11, 2023

Robotic Control for Vibration Reduction of Swinging Products

1st Robbert van der Kruk
Control Systems Technology
University of Technology
Eindhoven, The Netherlands
r.j.v.d.kruk@tue.nl

2nd Arend Jan van Noorden
Mechatronic System Development
ASML
Veldhoven, The Netherlands
aj.van.noorden@gmail.com

3rd Tom Oomen
Control Systems Technology
University of Technology
Eindhoven, The Netherlands
t.a.e.oomen@tue.nl

4th Rene van de Molengraft
Control Systems Technology
University of Technology
Eindhoven, The Netherlands
m.j.g.v.d.molengraft@tue.nl

5th Herman Bruyninckx
Control Systems Technology
University of Technology
Eindhoven, The Netherlands
h.p.j.bruyninckx@tue.nl

[1]

***Abstract*—Input shaping can effectively reduce residual vibrations of flexible systems induced by the reference signal. For the control of cranes, the usefulness of input shaping is well known and implemented. For robotic placement applications the shaped reference trajectory could result in a reduced overall settling time. Both a frequency domain an time domain view is presented of the input shaping process of a position controlled robot driven flexible system. A trade off is required of the move time of the reference versus overshoot. In this paper a method is introduced to relate the relative overshoot to the ratio of vibration time and move time. This enables the selection of the highest possible acceleration value to meet the overshoot specification.**

For fast robotic pick and placement of swinging products input shaping provides significant reduction of the overshoot, without settling time loss, when the move time equals more than 60 percent and less than 80 percent of the natural vibration time. The classic zero vibration input shaper (ZV) provides best overall performance. When this shaper is combined with bandwidth matching of the joint servo controllers to the vibration frequency of the suspended product, comparable performance is obtained while providing a smoother acceleration of the object to reduce peel-off. An experimental validation on a delta robot system, confirms the performance improvement obtained by an input shaper for a cheese product packed in a liquid bag suspended by a vacuum suction cup gripper.

***Index Terms*—point-to-point trajectory generation, motion control, swinging products , suspended products , vibration reduction, food packaging, horizontal dynamic forces, pendulum dynamics, robotic pick and place, command shaping, input shaping , suction cup gripper**

I. Introduction

The productivity of the handling of products picked by vacuum grippers or other suspended means in the packaging industry is limited by unwanted residual vibrations and transient deflections. The pick and place actions are often driven by servo controllers in industrial robots or dedicated equipment. A knowledge gap is noticed to effectively improve the positioning and throughput of these applications. This paper aims to provide a design method for the handling of these swinging products and place this in the context of point-to-point trajectory generation for the control of flexible mechanisms. The main contribution of this paper is the introduction of a well-described relation $u_0(\tau)$ of the placement accuracy u_0 and the relative vibration time τ of suspended products. This is used to design an input shaper feed forward controller. In this paper we build on the earlier work of (M. Smith, 1957), (Singer, Seering, 1990) and (Singhose, 2009) who created the framework of input shapers to apply typically for the vibration reduction in cranes. Here we explicitly study the performance contribution of input shapers for the robotic position control of swinging suspended objects, such as food products picked by vacuum suction cup grippers for packaging. The outline of this paper is as follows: In section II the related work is described to create the scientific context. State of the art trajectory generation methods are presented. Relevant input shaping methods to suppress vibrations originated from the reference are summarized. In section III performance criteria and control strategy are discussed to relate to practical objectives. In section IV the swinging product case is modelled as a pendulum and design rules for the acceleration to reduce overshoot are given. An experimental food packaging use case and its measurements is described in section V. The implementation aspects are discussed in section VI.

II. Background

A. Trajectory generation methods

Robots need to operate in unknown environments and so it is not sufficient to plan beforehand. They need to react to sensor information. In that case a trajectory needs to be generated in real time to execute the task within constraints like maximum acceleration, speed and workspace. The trajectory generation interpolates between waypoints and interfaces between the motion path and motion control to provide the reference position trajectory. A single endpoint or list of points with defined kinematic state serves as the task description. As a

[1]Preprint IEEE ICM 2023, Loughborough, UK 15-17 March 2023

result the online trajectory generation calculates a trajectory $r(t)$ to the new waypoint considering the constraints see (Kröger, Wahl, 2010). Third-order profiles which limit the jerk (JL) are typically used. To move a single distance,

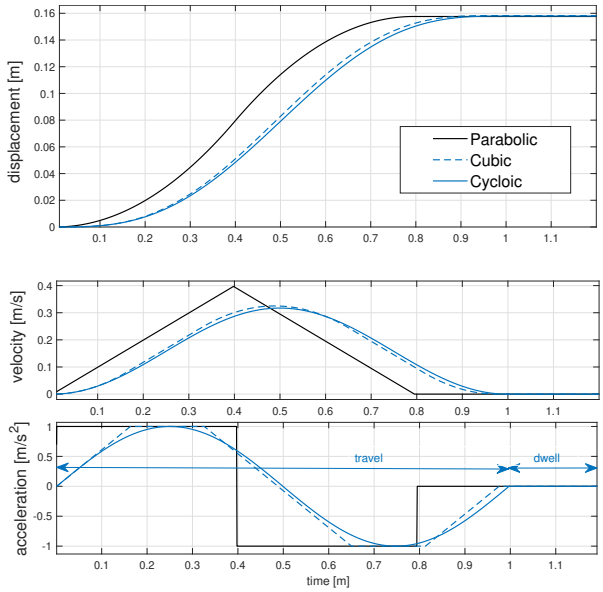

Fig. 1: Position, velocity and acceleration profiles for Parabolic, Cubic, and Cycloic point-to-point trajectories.

rest to rest, with constrained acceleration and deceleration is demonstrated in Figure 1. The parabolic position trajectory is S shaped, its velocity profile is triangular while the acceleration consists of a positive and a negative pulse. In this study, we ignore the constant velocity part of the trajectory since is has limited effect on the dynamics and it is not reached for fast pick and place moves. The topic of trajectory generation is related to the study of cam shaft profiles by (Kwakernaak, Smit, 1968) and (Koster, 1973) where cycloidal profiles are widely used. It's acceleration shapes are jerk-limited. Van der Hoek (1984) introduced the $u_0(\tau)$ diagrams to clarify the relation between positioning accuracy and the move time. The objective was the design of lightweight and highly rigid mechanisms in order to achieve high positional accuracy at high speeds. To compare reference profiles, $r(t)$ is usually expressed in polynomials of second , third or higher order. It is usually concluded that a limited 3rd derivative (jerk) results in an attractive response see Figure 1, but the jerk results also in a longer time to reach the top velocity and needs a higher maximum acceleration. This higher acceleration causes higher deformation and hence higher residual vibration. The jerk limited (JL) trajectory profiles are typically available in industrial digital servo controllers. It approaches the cycloid. In general high order profiles use more move time with equal acceleration constraints. For real-time applications the third order trajectory generators were introduced in the late eighties upon the availability of fast signal processors see (Van der Kruk, Scannell, 1988). Compared to the parabolic, the cubic profile needs a 50% higher value of acceleration for equal travel time. Often this effect is not addressed.

B. Frequency response of the reference trajectory

The frequency spectrum of the reference R(s) impacts the frequency response Y(s) of the Linear Time Invariant system G(s) by:

$$Y(s) = R(s) * G(s) \tag{1}$$

The acceleration profile of the reference a(t) can be described using the Heaviside step functions u(t) as follows:

$$a(t) = a_{max}(u(t) - 2u(t - T_{acc}) + u(t - 2T_{acc})) \tag{2}$$

The Laplace transform a(s) of a(t) is:

$$a(s) = \int_{t=0}^{\infty} a(t)e^{-st}dt = \frac{a_{max}}{s}(1 - 2e^{-T_{acc}s} + e^{-2T_{acc}s}) \tag{3}$$

and the Laplace transform of the position reference profile r(t) is:

$$r(s) = \frac{a(s)}{s^2} = \frac{a_{max}}{s^3}(1 - 2e^{-T_{acc}s} + e^{-2T_{acc}s}) \tag{4}$$

In the same way using Heaviside step functions and Laplace transformation, the Laplace transforms of the cycloid and cubic profiles can be obtained. The amplitude part of the Bode diagrams of their acceleration profiles a(s) is depicted in Figure 2.

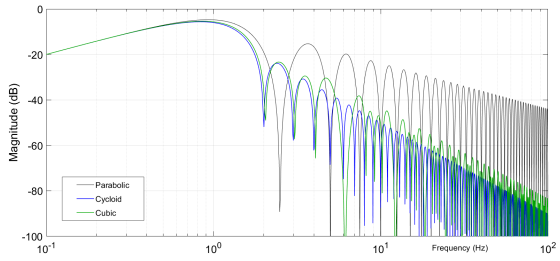

Fig. 2: Bode amplitude diagrams a(s) of Parabolic, Cubic and Cycloic trajectories. $a_{max} = 1$ m/s^2. The move time of 1 s corresponds to the maxima at 1 Hz.

High frequency modes are visible and originate from the pulse shaped second en third derivatives. For rest-to-rest motions the higher derivatives are discontinuous at the start and end. The high frequency modes are the most significant for the parabolic. The cycloid trajectory has the lowest high frequency modes but at the price of a longer travel time. High frequency modes are typically suppressed in the trajectories by using a value of the jerk time corresponding to a time constant related of the frequency range of interest.

C. Input shaping

When recognized that the main disturbance is not external but by the trajectory itself, input shaping provides a way to reduce the vibration frequency from the reference. Figure 3 depicts the frequency spectrum of a pendulum excited by a parabolic trajectory and the same spectrum input shaped. Input shaping is based on linear system theory and is a time

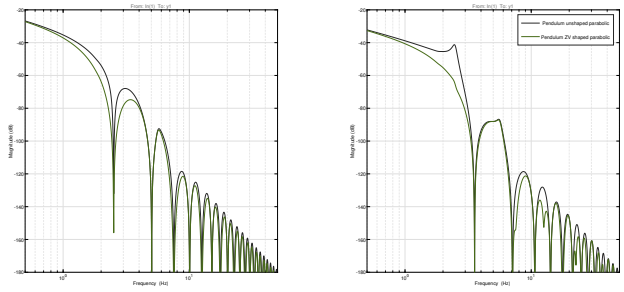

(a) $\tau = 0.5$ (b) $\tau = 0.71$

Fig. 3: Frequency spectra of a linearised pendulum transfer function excited by a parabolic trajectory (black) and input shaped parabolic (green)

domain based. The residual vibration is reduced by generating an input that cancels its own vibration. The simplest self canceling input consists of two impulses (Posicast or ZV shaper (M. Smith, 1957) and (Singer, Seering, 1990) . The first impulse starts the system vibrating, the second impulse is delayed by one half period of the vibration period. The vibration caused by the second impulse is out of phase with the first vibration, thereby canceling it. Because impulses cannot be used to move physical systems, the two impulses, also known as the input shaper, must be convolved with a physically realizable input. The shaped input that results from the convolution will have the same vibration-canceling properties as the input shaper. Input shaping methods use superposition of delayed parts of the original profile such that the steady state position equals the original end position. For flexible systems such as cranes, they are reported to reduce low-frequency vibration modes (Singhose, 2009). The classic zero vibration method (ZV) suppresses a harmonic vibration by delaying a fraction (k/k+1) of the reference signal by half the period of damped vibration T_d to add it to the remaining fraction (1/(k+1) of the original reference. Its two parameters k and T_d are prescribed by:

$$k = \exp\frac{-\zeta\pi}{\sqrt{1-\zeta^2}} \quad , \quad T_d = \frac{2\pi}{\omega_n\sqrt{1-\zeta^2}} \tag{5}$$

The natural frequency of the vibration equals ω_n. ζ is the damping ratio of the vibration. For swinging type of objects its value is often less than a several % and hence the value of k is close to 1, which means that both gain factors of the ZV filter are close to 1/2. The discrete time (sample time T_s) version of the ZV transfer function is from $r_s(n)$ to $r(n)$:

$$r_s(n) = \frac{1}{k+1}r(n) + \frac{k}{k+1}r(n-n_d) \tag{6}$$

$$n_d = \left[\frac{T_d}{2T_s}\right]. \tag{7}$$

The Extra Insensitive (EI) method is described by (Singhose et al., 1994) and (Conker et al., 2016). It uses an additional

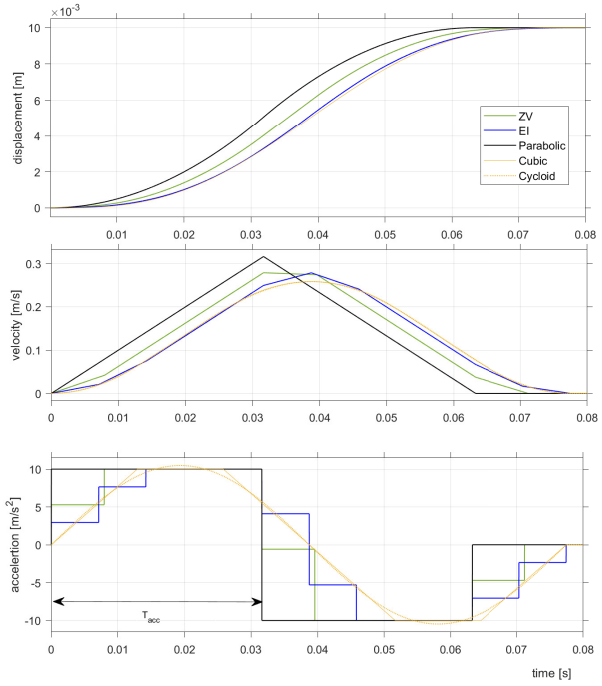

Fig. 4: Comparison of parabolic, cubic (JL), cycloid trajectories and ZV and EI input shaped parabolic.

branch with a full delay of T_d. Unlike the ZV shaper it does not attempt to force the vibration to zero.

$$V_{tol} = 0.05, k_1 = (1+V_{tol})/4, k_2 = 1-k_1-k_3, k_3 = k_1 \tag{8}$$

$$r_s(n) = k_1 r(n) + k_2 r(n-n_d) + k_3 r(n-2n_d) \tag{9}$$

A small level of vibration V_{tol}%is allowed at the modeling frequency and the insensitivity to modeling frequency errors is enhanced. Its parameters are given inConker et al. (2016) . The jerk limiting input shaper (JL) can be created by a Finite Impulse Response (FIR) filter applied to the second order trajectory or by direct generation. It has one parameter: the jerk time T_j or the jerk j [$\mathrm{m/s^3}$], which is the first time derivative of the acceleration:

$$T_j = \frac{a_{max}}{j} = T_d \tag{10}$$

The JL filter transfer function is described in Béarée (2014). Here we give the discrete time equation :

$$r_s(n) = r_s(n-1) + \frac{T_s}{T_j}[r(n) - r(n-n_j)], \tag{11}$$

$$n_j = \left[\frac{T_j}{T_s}\right] \tag{12}$$

Input shaping of the parabolic reference results in pulsed acceleration profiles for ZV and EI as depicted in Figure 9. This differs from the smooth acceleration profile of the cycloid and cubic (JL) . The frequency responses are plotted in Figure 5. The magnitude plot shows stop bands around the natural frequency F_d: the natural vibration is suppressed. The EI

shaper has the widest stop band at the price of a full vibration cycle time delay T_d see tableI. The ZV and EI shapers show a zero phase delay at F_d and all its harmonics. The JL input shaper has a wider stop band than the ZV shaper but smaller than the EI input shaper and at the price of a full vibration cycle time delay.

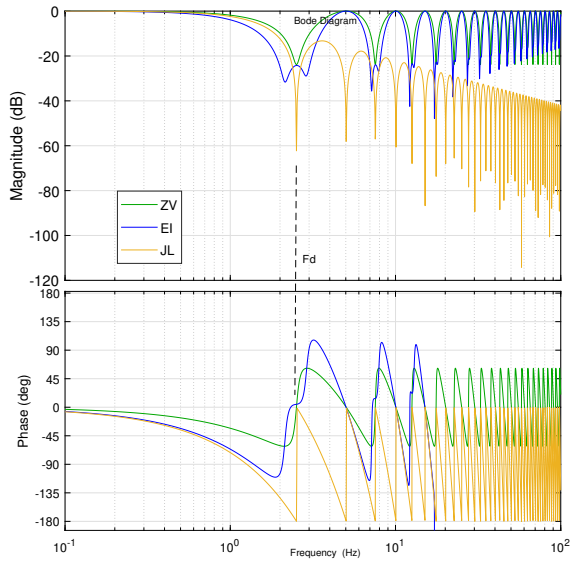

Fig. 5: Frequency response of the input shape ZV, EI and JL. The damped natural frequency F_d is suppressed. The ZV and EI shapers also suppress the odd harmonics, while the JL shaper suppresses all harmonics.

The negative shapers as reported by Lau, Pao (2001) and Singhose et al. (1996) reduce the length of the shaper (the move time) significantly. Their disadvantage is the excitation of high frequency modes and the lack of guarantees for the shaped input signal. Further details on the comparison of methods of residual vibration reduction are provided by Singhose, Pao (1997). Conventionally designed frequency domain filters such as notch and low pass filters are never better than the mentioned input shapers as proved by Singhose, Vaughan (2011).

III. Performance criteria and control strategy

To distinguish the differences in input shapers, trajectories and controllers performance criteria are needed. The measurements needed are part of the control strategy. The position accuracy in terms of overshoot is related to the reference move time T_m. The vibration amplitude of the swinging object should be less than specified to avoid collision and inaccurate placement. Using the notation in (Van der Hoek, 1984) we define:

$$u_0 = \frac{\max|r - x(t)|}{r}, \quad t > T_m \tag{13}$$

$$\tau = \frac{T_d}{T_m} \tag{14}$$

$x(t)$ is the position of the object. r is the reference end position. The overshoot percentage u_0 is related to the dimensionless natural vibration time τ which is the ratio of the damped vibration time T_d and the reference travel time T_m. Table I lists these τ values for the input shapers. The relationship $u_0(\tau)$ for a one mass spring damper is described in Koster (1973). For a parabolic the relation is quadratic: $u_0 = 0.04\tau^2$. Doubling the travel time results in an overshoot reduction of four. For the cycloid the relation is: $u_0 = 0.06\tau^3$ which is highly favourable over the parabolic when $\tau < 0.4$ see Figure 6. The importance of the $u_0(\tau)$ relation is that for a given overshoot and vibration time a maximum value of τ is found. Hence if the controller bandwidth $1/T_d$ is fixed, the minimum value of the acceleration time is defined. It also prescribes the controller bandwidth for a given overshoot and acceleration time. Huey

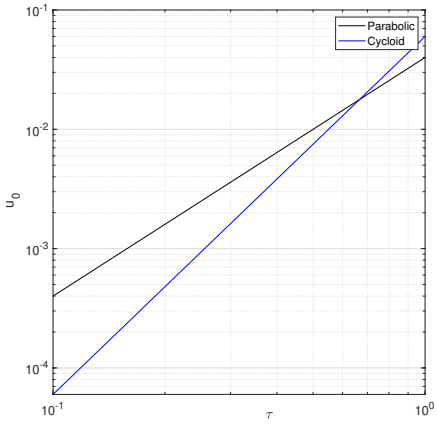

Fig. 6: Relative overshoot for parabolic and cycloid point-to-point trajectories with optimal damping for a one mass spring damper system

(2006) concludes that the concurrent input shaper and PD feedback control results in superior controllers for the one mass spring damper systems when the design constraints do not force an over-damped system. The input shapers reduces the overshoot towards zero while the feedback controller reduces the non-linearity's, disturbances and modelling errors. The $u_0(\tau)$ relations will be derived in the next section to conclude on the superiority hypothesis of the combined PD feedback control and input shaper for these systems. The position of the product x is typically not measured during the pick and place process. For localisation a sensor tag attached to it could be used to tune the controller. The control scheme in Figure 7 shows the controlled variable x, which is not measured directly but estimated from a secondary measurements q, the actuator positions. The feedback controller C eliminates disturbances such a load changes and friction. x is called an inferential variable since it is not directly expressed, as defined by (Oomen et al., 2015) for motion systems. The measured values q, which are the estimated values of the controlled variable x, is compared against the input shaped reference and the control action C is taken.

TABLE I: Reference trajectories and acceleration times. T_d : damped natural vibration time, T_{acc} : acceleration time of the parabolic profile

Trajectory and input shaper	Move time T_m	τ
Parabolic (unshaped)	$2T_{acc}$	$\frac{T_d}{2T_{acc}}$
Parabolic & ZV	$2T_{acc} + T_d/2$	$\frac{T_d}{2T_{acc}+T_d/2}$
Parabolic & EI	$2T_{acc}$ + T_d	$\frac{T_d}{2T_{acc}+T_d}$
Parabolic & JL	$2T_{acc}$ + T_d	$\frac{T_d}{2T_{acc}+T_d}$

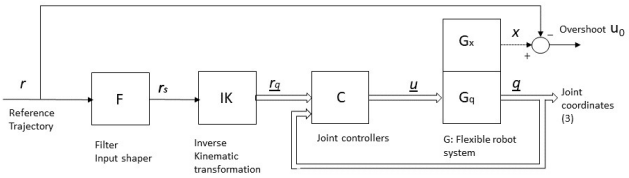

Fig. 7: Robotic Control structure with indirect control. The dashed line indicates that the performance output x is not measured during operation. Gq and Gx : transfer functions

IV. Robotic pick and place of swinging products

Robotic packaging includes often fast pick and place cycles of suspended food packages. When suction cups are used the suspended product turns into a swinging load when moved. Suction cups grippers are widely used in the packaging industry to pick and place products from conveyor belts in boxes. The grip is firm in case of no leakage in the vacuum system but unwanted transient deflection and residual vibration could occur resulting in problems with accuracy and throughput. For a physical model of the robot manipulator and the product, we consider the robot end-effector as a position controlled cart which moves in the horizontal direction and a load which rotates in the vertical plane. The horizontal movement of the load $x(t)$ is observed and expected to meet the positional requirement see Figure 8.

The following assumptions are made throughout: The load and cart are connected by a mass-less and rigid link. The cart moves along the x-axis only. The positions $x(t)$ and $q(t)$ can be measured. Cart and load are considered as known point masses. The effects of disturbances are neglected. The viscous damping (D_m) can be estimated from the amplitude reduction of a free vibration response of the product. The equations of motion of the horizontal movement of the object (m) are based on a pendulum driven by the mass M as depicted in Figure 8 with two independent coordinates q and θ. The horizontal movement of m depends on these two coordinates according to (18). The position controlled motion of the cart is modelled by a spring K_p and a damper K_v to model a digital PD controller, which is frequently used in industrial robots. This pendulum system for pick and place applications is an underactuated system: the number of actuators is less than the degree of freedom of the system. In this case the degree of freedom is two (i.e. position of the end effector q and position of the object x), but the number of actuators is one. The bandwidth ω_c and relative damping β_c of the position controlled cart are:

$$\omega_c = \sqrt{\frac{K_p}{(M+m)}}, \quad \beta_c = \frac{K_v}{2\sqrt{K_p(M+m)}} \tag{15}$$

Lagrange equations lead to the differential equations of

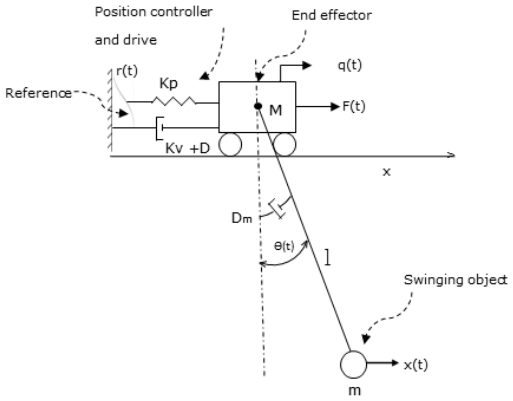

Fig. 8: Abstraction of the handling of a swinging product picked by a suction cup: A suspended pendulum driven by a position controlled cart

motion (Ho Duc et al., 2014), (Conker et al., 2016). In this case for the position controlled cart pendulum model of Figure 8 are:

$$K_p(r-q)-(K_v+D)\dot{q} = (M+m)\ddot{q}+ml\ddot{\theta}\cos(\theta)-ml\dot{\theta}^2\sin(\theta) \tag{16}$$

$$ml\ddot{q}\cos(\theta) + ml^2\ddot{\theta} + D_m\dot{\theta} + mlg\sin(\theta) = 0 \tag{17}$$

$$x = q + l\sin(\theta) \tag{18}$$

The natural frequency of the vibration of the product can be obtained from (16) by neglect of the damping D and D_m at small values of θ:

$$\omega_n = \sqrt{\frac{g(M+m)}{Ml}} \approx \sqrt{\frac{g}{l}} \quad (m \ll M) \tag{19}$$

From (16), (17) and (18) simulations of the responses of the load position for parabolic and input shaped parabolic were collected. No further simplification or linearisation is carried out to avoid reduced accuracy as described by Burg et al. (1996).

Typically the joint controllers of the robot are tuned for a fast and accurate response with high servo stiffness of the end effector resulting in a bandwidth higher than the vibration frequency of the load. Hence the controlled robot is considered here as a rigid body. The term $m\ddot{q}\cos(\theta)$ in (17) represents the inertial force transmitted to the pendulum mass m and

is usually high at the moment the acceleration switches to deceleration. To provide additional damping of the pendulum, we match the bandwidth of the controller to the frequency of vibration $\omega_c = \omega_n$ with relative controller damping $\beta_c = 1$. As a result the servo stiffness and servo damping are reduced to:

$$K_p = \omega_n^2(M+m), \quad K_v = 2\omega_n(M+m). \tag{20}$$

The input shaper ZV combined with this matched impedance we name ZV&IM in the sequel.The simulation results of the relative overshoot as a function of τ are depicted in Figure 9 to provide the trade off between overshoot accuracy and move time.

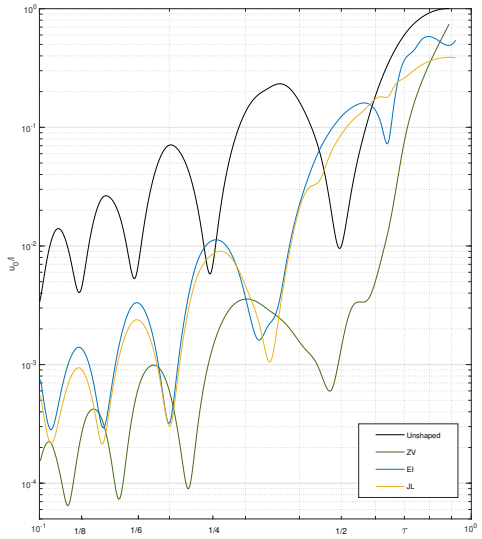

Fig. 9: Relative overshoot u_0/l and as a function of τ for parabolic trajectory and ZV, EI and JL input shapers

From reference move time, the acceleration T_{acc} is set to realise τ using: the values in table I with known vibration period T_d. The overshoot is constrained by the length l. At $\tau = 1/2, 1/4, 1/6, ...$ the velocity of the pendulum approaches zero, the reference acceleration switches to deceleration resulting in a minimal swing in the dwell period. This behaviour was also exactly described by Van der Hoek (1984, chap. 8) [2]. In the range $\tau < 0.4$ all input shapers reduce the overshoot significantly. Here the move time is much larger than the vibration time such that the end-effector motion is dominant and only a low level of vibration is excited. In the interval $0.4 < \tau < 0.6$ the EI and JL input shapers do not contribute to overshoot reduction. For $\tau > 0.6$ the move time approaches the vibration period and results in high speed. The ZV input shapers reduce the overshoot significantly for values of $\tau < 0.8$ at a factor of almost 10. The EI and JL input shapers reduce the overshoot as well but not as strong as the ZV shaper. As a typical use case we consider the system as tabulated in II. Figure 10

[2]A dedicated natural trajectory could be generated based on this behaviour since the acceleration time should be an integer number of the damped vibration time.

TABLE II: System parameters for swinging product, position driven by a robot system

Parameter	Symbol	Value	Unit
Mass product	m	0.2	Kg
Mass end effector	M	10	Kg
Equivalent length of load	l	0.04	m
Natural frequency product	Fn	2.57	Hz
Damping ratio product	ζ	0.041	-
Travel	r	0.3	m
Sample time	Ts	0.001	s
Bandwidth position controller	f_c	15	Hz
Relative damping controller	β_c	0.7	-

demonstrates the vibration reduction of the ZV input shaper when $\tau = 0.73$ The responses of the input shapers ZV, JL and

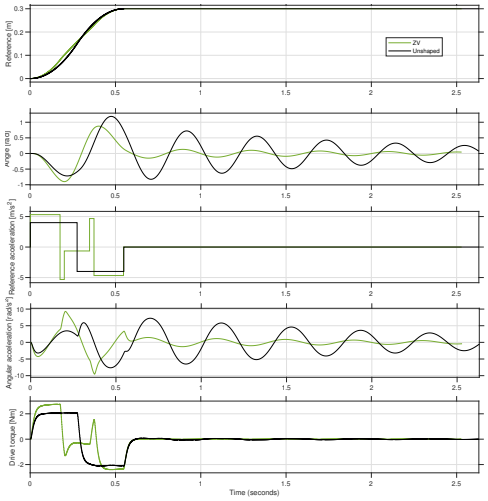

Fig. 10: Reference, Angle, Reference acceleration, Angular acceleration and Drive torque for ZV shaped and unshaped parabolic trajectories. $\tau = 0.73$

ZV&IM with equal travel time ($\tau = 0.7$) are plotted in Figure 11. The unshaped response is hardly damped and results in vibrations approaching the amplitude l, the equivalent length of the load. The ZV has the highest overshoot reduction (9 times). The sensitivity of relative overshoot to variations of the equivalent pendulum length l are plotted in Figure 12. The ZV shaper has the lowest overshoot when tuned well in case of small variations. Within the range of 10 percent variations the ZV shaper features the highest suppression. In the range of 10 to 20 percent the ZV shaper performs best when the bandwidth of the robot servo controllers are matched to the vibration frequency of the system. The EI shaper is reported to provide better insensitivity for larger variations Singhose et al. (1994).

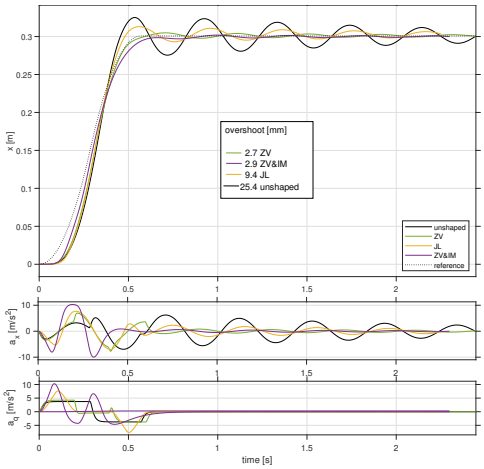

Fig. 11: Displacement, product acceleration and actuator acceleration responses for parabolic shaped trajectories. Simulation results. Parameters in Table II. Frequency well tuned, damping mismatch 10%, $\tau = 0.7$

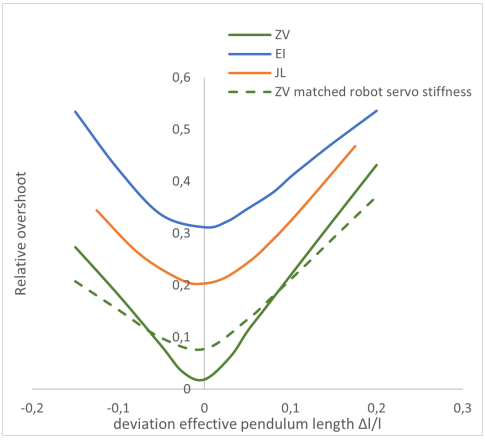

Fig. 12: Sensitivity of overshoot to variations of the equivalent pendulum length for ZV, EI, JL and ZV combined with matched robot servo stiffness

V. Experimental results from food packaging use case

The industrial packaging of sealed food into a case is typically executed by fast delta robots whose paths can be programmed to stack the products identified by a fixed camera at the entry of the conveyor belt, see Figure 13. Compliant vacuum grippers or suction cups are used which deform to match the product shape of the sealed food. An example of a viscous product is a fluid bag is demonstrated in Figure 14. These applications are high-volume and include the case packaging of soup in a plastic enclosure. The throughput limitation of the point to point movements is caused by the peel-off of from the suction cups and the oscillations during placement. If the breakaway force between the lip of the vacuum gripper exceeds the grippers retention force, the product peels off. Inaccurate placement or collision with the box by overshoot can result in damaged products or misplacement causing the prescribed number of products in the box will not be met. It is shown by Noorden van (2021) that the vacuum gripped products behave as a pendulum and can be modelled so accurately. The product variations are limited within batches. The unloaded delta robot shows two resonance frequencies in the range of 32 to 70 Hz in all directions. They are caused by the coupling of the drives and the stiffness of the upper arm. The product vibration frequency is in the range of 2 to 2.8 Hz, significantly larger than the lowest robot resonance frequency so the controlled robot mechanism is modelled as a rigid body as depicted in Figure 8. The vibration period of the product depends on the combination of the gripper and the product since both influence the length. Figure 14 depicts the cheese product in fluid in a bag picked by the suction cup (red) coupled to the robot end-effector (blue). To detect the displacement a visual fiducial system attached to the front of the bag is used. The 3D pick and place path is defined by 4 user defined positions P0 to P3 see Figures 13 and 15 The straight lines are connected by blends to create a smooth path by B-splines. The 3D task oriented coordinate system needs the inverse kinematic transform to create the joint displacements every 1 ms. Input shaping is in task coordinates. Figure 16 plots the experimental results for a parabolic and its ZV shaped trajectories. Note that the acceleration of the product centre (PCP) is reduced by almost a factor of two. To investigate the ZV shapers performance in a production environment, a use case test was executed: The placement inside a box within an overshoot less than 15mm. A two fold decrease in travel time at the expense of slightly higher product accelerations was found when x and z axes were input shaped during motion. To find the travel time decrease until the product starts to peel off, a maximum horizontal PCP acceleration of 20 $\mathrm{m/s^2}$ was imposed. This resulted in a 14% decrease in travel time and vibration reduction of 32%. The τ value for these test was only 0.4 indicating potential for further improvement see Figure 9. Synchronization is needed to conserve the original reference path. Shaping the x-axis only gives a minimal result, since the suction cup is a coupled mechanism. Different travel times between axis could be equalized by delaying the axis taking the longest travel time.

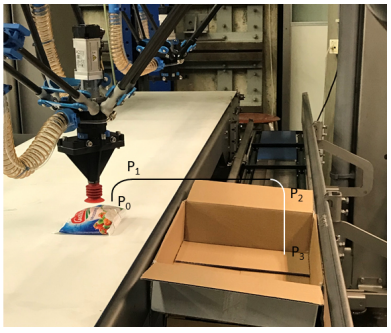

Fig. 13: Delta robot setup and path for pick and placement of food-packaging. Source Blue Print Automation Woerden, The Netherlands.

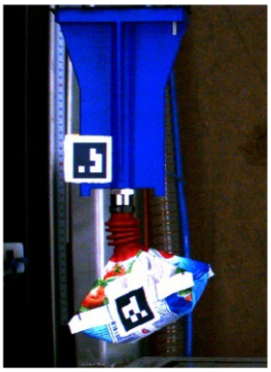

Fig. 14: Swinging packed viscous product in fluid picked by suction cup. Source Blue Print Automation, Woerden, The Netherlands

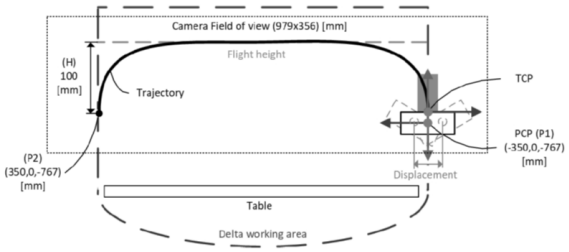

Fig. 15: 2D view of the path to test the dynamic behaviour of the product centre point (PCP). TCP is the robot tool centre point.

VI. Implementations aspects

Input shapers can be represented as the sum of time delays which sum of coefficients equals 1 see (5). It is a Finite Impulse Response (FIR) filter and does not require knowledge of the reference in advance. It is executed every sample time T_s of the trajectory generation and is located in the information path after the trajectory generator output r and before the inverse kinematic coordinate transformation to the joint position controllers. Such the input shaper is a clear feed forward control method. It can be implemented independent from trajectory generator and position controllers. The upper non-delayed path transmits a fraction of the reference and the delayed ($T_d/2$ seconds) lower path transmits the remaining part. The number of delay tabs equals the nearest integer of T_d/T_s, which could be very high! Tuning of the delays and gains is realised by measuring the damped vibration period and its decay in time. A typical value for the trajectory generator sample time T_s is 1 ms, which is also sufficient for the input shaping of frequencies in the range to 10 Hz.

The travel time delay created by input shaping causes synchronisation errors between other axes of the planned path. This can be solved by delaying the other trajectories or shaping all directions equally. Navarrete et al. (2015) described the tracking and synchronization of two accurate scanning stages. They propose to augment the master stage filters with the zeros from the slave stage and reversely. The feasibility was confirmed by simulation results and, to some extend, by measurement results obtained from an industrial wafer scanner.

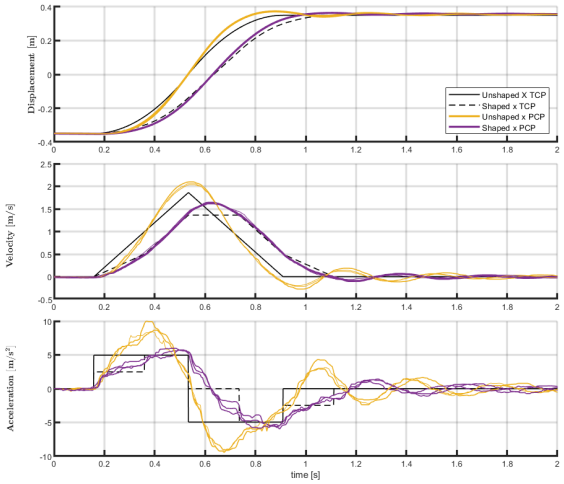

Fig. 16: Measured displacement, velocity and acceleration of unshaped and shaped responses. Maxima, minima and modus response values at $\tau = 0.4$

VII. Conclusion

This paper shows that for fast robotic control of swinging products, input shapers contribute to reduce the overshoot without overall move time delay for point-to-point movements. It is argued that the implementation of the input shapers is straightforward and independent of the reference trajectories. The ratio of vibration time and move time τ has a major influence on the overshoot. Trade-off relations of the relative overshoot as a function of τ) for the relevant input shapers have been derived for robotic pick and place positioning of swinging products. With known allowable overshoot and travel, the highest possible move time can be obtained from these curves.

For fast robotic pick and placement of swinging products input shaping provides a method to significantly reduce of the overshoot, comparing equal reference move times. A typical pick and place application requires a vibration time over travel time ratio in the reach of $0.6 < \tau < 0.8$. For these movements the maximum acceleration of the trajectory generator in product space coordinates should be set accordingly to meet the required displacement and move time. In that case overshoot reduction in the range of 5 to 10 is possible.

The zero vibration input shaper ZV provides best overall performance. Combined with matching the servo controller bandwidth frequency of the joint to the vibration frequency comparable comparable performance is obtained while providing a smoother acceleration of the products to reduce transient reflections. An experimental validation on a delta robot system confirms the reduction and peel off obtained by a ZV input shaper for a cheese product packed in a liquid bag suspended by means of a suction cup. All product space axes need to be are synchronised to avoid overshoot in other directions.

Within the range of 10 percent equivalent length variations

the ZV shaper features the highest suppression. In the range of 10 to 20 percent variations the ZV shaper performs best when the bandwidth of the robot servo controllers are matched to the vibration frequency of the system. Jerk limited (JL) third order reference trajectories can be regarded as input shaped second order reference trajectories. Its performance is inferior to ZV shapers, but can be used effectively to reduce a range of high frequency modes.

VIII. Acknowledgments

This research is supported by grants of Netherlands Organization for Scientific Research NWO/TTW in the Netherlands as part of the project Cognitive Robotics for Flexible Agro-Food Technology (FlexCRAFT) the bibitems directly in the

References

Burg T., Dawson D., Rahn C., Rhodes W. Nonlinear control of an overhead crane via the saturating control approach of Teel // Proceedings of IEEE International Conference on Robotics and Automation. 4. 1996. 3155–3160 vol.4.

Béarée Richard. New Damped-Jerk trajectory for vibration reduction // Control Engineering Practice. 07 2014. 28. 112–120.

Conker Caglar, Yavuz Hakan, Bilgic Hasan Huseyin. A review of command shaping techniques for elimination of residual vibrations in flexible-joint manipulators // Journal of Vibroengineering. aug 2016. 18, 5. 2947–2958.

Ho Duc Tho, Nguyen Hung, Nguyen Quoc Chi. Input shaping Control of an Overhead Crane // VCM. 11 2014.

Huey John R. The Intelligent Combination of Input Shaping and PID Feedback Control. 2006.

Koster M.P. Vibrations of cam mechanisms and their consequences on the design. 1973.

Kröger Torsten, Wahl Friedrich M. Online Trajectory Generation: Basic Concepts for Instantaneous Reactions to Unforeseen Events // IEEE Transactions on Robotics. 2010. 26, 1. 94–111.

Kwakernaak H., Smit J. Minimum Vibration Cam Profiles // Journal of Mechanical Engineering Science. 1968. 10, 3. 219–227.

Lau Mark, Pao Lucy. Comparison of input shaping and time-optimal control of flexible structures // ACC. 2. 02 2001. 1485 – 1490 vol.2.

M. Smith Otto J. Posicast Control of Damped Oscillatory Systems // Proceedings of the IRE. 1957. 45, 9. 1249–1255.

Navarrete Miguel Ochoa, Heertjes Marcel F., Munnig Schmidt Robert H. Common zeros in synchronization of high-precision stage systems // 2015 IEEE International Conference on Mechatronics (ICM). 2015. 602–607.

Noorden A.C.H. van. Delta Robot Motion Stabilization for Flexible Packaging of Viscous Fluid Products in a Bag. 2021.

Oomen Tom, Grassens Erik, Hendriks Ferdinand. Inferential Motion Control: Identification and Robust Control Framework for Positioning an Unmeasurable Point of Interest // IEEE Transactions on Control Systems Technology. 2015. 23, 4. 1602–1610.

Singer N. C., Seering W. P. Preshaping Command Inputs to Reduce System Vibration // Journal of Dynamic Systems, Measurement, and Control. 03 1990. 112, 1. 76–82.

Singhose W.E., Singer Neil, Inc Convolve, Seering Warren. Design And Implementation Of Time-Optimal Negative Input Shapers // https://www.researchgate.net/publication/2584317. 03 1996.

Singhose W.E., WP Seering, Singer Neil. Residual Vibration Reduction Using Vector Diagrams to Generate Shaped Inputs // Journal of Mechanical Design. 06 1994. 116.

Singhose William. Command Shaping for flexible Systems: A Review of the First 50 years // International Journal of precision engineering and manufacturing. oct 2009. 10, 4. 153–168.

Singhose William, Pao L. A comparison of input shaping and time-optimal flexible-body control // Control Engineering Practice. 1997. 5, 4. 459–467.

Singhose William, Vaughan Joshua. Reducing Vibration by Digital Filtering and Input Shaping // IEEE Transactions on Control Systems Technology. 2011. 19, 6. 1410–1420.

Van der Hoek W. Het voorspellen van het dynamisch gedrag en positioneernauwkeurigheid van constructies en mechanismen. 1984. 4004007200001.

Van der Kruk Robbert, Scannell John. Motion Controller employs DSP technology // Official Proceedings of the Twelfth International MOTOR-CON Conference Munich, West Germany. VI 1988. 183–196.

Nomenclature

β_c	Relative damping controller [-]
ω_c	Controller bandwidth [rad/s]
ω_n	Natural vibration frequency [rad/s]
τ	Dimensionless vibration time [-]
r	Reference [m]
T_{acc}	Acceleration time [s]
T_d	Damped vibration time [s]
T_j	Jerk time [s]
T_m	Reference move time [s]
T_s	Controller sample time [s]
u_0	Relative overshoot [-]
l	Equivalent length of load [m]